

Planetesimal-driven migration as an explanation for observations of high levels of warm, exozodiacal dust

Amy Bonsor,^{1,2★} Sean N. Raymond,^{3,4} Jean-Charles Augereau¹ and Chris W. Ormel⁵

¹*UJF-Grenoble 1 / CNRS-INSU, Institut de Planétologie et d'Astrophysique de Grenoble (IPAG) UMR 5274, F-38041 Grenoble, France*

²*School of Physics, H. H. Wills Physics Laboratory, University of Bristol, Tyndall Avenue, Bristol BS8 1TL, UK*

³*CNRS, UMR 5804, Laboratoire d'Astrophysique de Bordeaux, 2 rue de l'Observatoire, BP 89, F-33271 Floirac Cedex, France*

⁴*Observatoire Aquitain des Sciences de l'Univers, Université de Bordeaux, 2 rue de l'Observatoire, BP 89, F-33271 Floirac Cedex, France*

⁵*Astronomy Department, University of California, Berkeley, CA 94720, USA*

Accepted 2014 April 9. Received 2014 April 8; in original form 2013 December 20

ABSTRACT

High levels of exozodiacal dust have been observed in the inner regions of a large fraction of main-sequence stars. Given the short lifetime of the observed small dust grains, these ‘exozodis’ are difficult to explain, especially for old (>100 Myr) stars. The exozodiacal dust may be observed as excess emission in the mid-infrared, or using interferometry. We hypothesize that exozodi are sustained by planetesimals scattered by planets inwards from an outer planetesimal belt, where collision time-scales are long. In this work, we use N -body simulations to show that the outward migration of a planet into a belt, driven by the scattering of planetesimals, can increase, or sustain, the rate at which planetesimals are scattered from the outer belt to the exozodi region. We hypothesize that this increase is sufficient to sustain the observed exozodi on Gyr time-scales. No correlation between observations of an outer belt and an exozodi is required for this scenario to work, as the outer belt may be too faint to detect. If planetesimal-driven migration does explain the observed exozodi, this work suggests that the presence of an exozodi indicates the presence of outer planets and a planetesimal belt.

Key words: methods: numerical – planets and satellites: dynamical evolution and stability – planets and satellites: general – zodiacal dust – planetary systems – infrared: planetary systems.

1 INTRODUCTION

Emission from dusty material is commonly observed in the outer regions of planetary systems. *Herschel* observations of solar-type stars find that 20 per cent have excess emission associated with a debris disc (Eiroa et al. 2013). This presents an increase from the ~ 16 per cent of stars found by *Spitzer* (Trilling et al. 2008). *Spitzer* detected similar excess emission, from warmer dusty material, around less than 1 per cent of stars at $8.5\text{--}12\ \mu\text{m}$ (Lawler et al. 2009). Detailed modelling of many systems find that the emission is likely to originate from multiple cold and warm components (e.g. Su et al. 2009; Churcher et al. 2011b). This could be compared to our Solar system, with its dusty emission from both the Kuiper and asteroid belts, as well as zodiacal dust in the terrestrial planet region.

In general cold, outer debris discs can be explained by the steady-state collisional grinding of large planetesimals (Dominik & Decin 2003; Wyatt & Dent 2002; Wyatt 2008). However, there exists a maximum level of dust that can be produced in steady state (Wyatt

et al. 2007a). Many of the warmer dusty systems exceed this limit (Absil et al. 2006; Wyatt et al. 2007a; Bonsor, Augereau, & Thébault 2012). The observed small dust has a short lifetime against both radiative forces and collisions. The origins of the high levels of warm dust are not fully understood. It is these systems that are the focus of this work. The term exozodi is commonly used to refer to systems with high levels of warm dust in the inner regions, referring to the similarity in location of the dust with our Solar system’s zodiacal cloud.

There are two main techniques that can be used to probe high levels of warm dust in the inner regions of planetary system, with distinct abilities to detect dust with different properties. Warm emission has been detected in the mid-infrared, for example using *Spitzer/IRS/Akari/WISE*, from very bright, dusty systems. Near- and mid-infrared interferometry, on the other hand, can probe closer to the star and detect lower levels of hotter dust. Together these observations build a picture of complex, diverse planetary systems in which dusty emission from the inner regions is common and in many cases has a complex structure, for example the dust may be split into various different belts (e.g. Lebreton et al. 2013; Su et al. 2013). In this work, we focus on improving our understanding of any system in which high levels of exozodiacal dust are observed that cannot be explained by steady-state collisional evolution.

*E-mail: amy.bonsor@gmail.com

The detection statistics resulting from the mid-infrared observations are very different to those from interferometry, mainly due to the differences in sensitivities of the two techniques and the two different populations probed. Both *Spitzer* and *WISE* found that emission from dust at 8.5–12 μm (Lawler et al. 2009) and 12 μm is rare (Kennedy & Wyatt 2013), occurring for less than 1 per cent of stars (*Spitzer*) or less than 1 in 10 000 (*WISE*, specifically emission from BD+20307-like systems). Interferometry has the advantage of being able to readily distinguish emission from the star and emission external to the star. A recent survey using The Center for High Angular Resolution Astronomy (CHARA)/Fiber Linked Unit for Optical Recombination (FLUOR) found excess emission around 18_{-5}^{+9} per cent of a sample of 28 nearby FGK stars with ages greater than 100 Myr (Absil et al. 2013). Although the constraints on the position, composition and distribution of the dusty material are poor, Bayesian analysis has found in a handful of cases that the emission most likely originates from small (less than μm) grains within 1–3 au (Absil et al. 2006; di Folco et al. 2007; Defrère et al. 2011). Ertel et al. (in preparation) find a similarly high occurrence rate for exozodiacal dust in *H* band, using Precision Integrated-Optics Near-infrared Imaging Experiment (PIONIER), a visitor instrument on the Very Large Telescope Interferometer.

Such high levels of small grains cannot be explained in steady state. One explanation that is regularly postulated is that we are fortunate enough to observe these systems during the aftermath of a single large collision (Lisse et al. 2009, 2012), maybe something like the Earth–Moon forming collision (Jackson & Wyatt 2012) or the aftermath of a dynamical instability similar to our Solar system’s Late Heavy Bombardment (Absil et al. 2006; Wyatt et al. 2007a; Lisse et al. 2012). Not only do such collisions occur rarely at the later times (>100 Myr) where exozodiacal dust is observed, but Bonsor, Raymond, & Augereau (2013b) show that, whilst high levels of dust are produced in the inner regions of planetary systems following instabilities, this dust is short-lived, and therefore, it is highly improbable that we observe such dust in more than 0.1 per cent of systems. On the other hand, Kennedy & Wyatt (2013) show that stochastic collisions could explain the distribution of (high) excesses observed with *WISE* at 12 μm . Whilst it is not clear whether the same explanation holds for both the handful of sources with high levels of excess emission in the mid-IR, and the ~ 20 per cent of sources with *K*-band excess detected using interferometry (Absil et al. 2013), it is clearly easier to find an explanation for the former.

A link with outer planetary systems has been hypothesized (Absil et al. 2006; Smith, Wyatt, & Haniff 2009; Wyatt et al. 2010; Bonsor, Augereau, & Thébault 2012). It has been shown that the emission could be reproduced in steady state by a population of highly eccentric ($e > 0.99$) planetesimals (Wyatt et al. 2010), but it is not clear how such a population could form. An alternative explanation could lie in the trapping of nano grains in the magnetic field of the star (Czechowski & Mann 2010; Su et al. 2013), but this still requires detailed verification. Most of the dust (>90 per cent) observed in our Solar system’s zodiacal cloud is thought to originate from the disruption of Jupiter Family Comets scattered inwards by the planets from the Kuiper belt (Nesvorný et al. 2010). Steady-state scattering in exoplanetary systems is not sufficiently efficient to sustain the high levels of dust observed in exozodi (Bonsor et al. 2012). We propose here that the efficiency at which planetesimals are scattered inwards by planets can be increased by the migration of a planet into an outer belt. We suggest that this could explain the high levels of exozodiacal dust observed in some planetary systems, in the manner illustrated by Fig. 1.

In the early evolution of our Solar system, Neptune is thought to have migrated outwards, due to an exchange of angular momentum as it scattered Kuiper belt objects (e.g. Fernandez & Ip 1984; Ida et al. 2000; Levison & Morbidelli 2003; Gomes, Morbidelli, & Levison 2004). This can explain some of the observed features of the Kuiper belt, including Pluto’s resonant, eccentric orbit (Malhotra 1993), or the ‘hot classical Kuiper belt’ (Gomes 2003). A similar exchange of angular momentum can occur between a planet and planetesimals in an exoplanetary system (e.g. Kirsh et al. 2009; Bromley & Kenyon 2011; Ormel, Ida, & Tanaka 2012). Such planetesimal-driven migration can occur in either an outward or an inward direction, at a rate and for a time-scale that depends on the properties of the disc and the planet (Kirsh et al. 2009; Ormel et al. 2012). We hypothesize that such planetesimal-driven migration can sustain the scattering of planetesimals into the inner regions of a planetary system on long time-scales. Such scattered planetesimals could account for the high levels of exozodiacal dust observed in some planetary systems, particularly in old (>100 Myr) planetary systems.

In this work, we use *N*-body simulations to consider when planetesimal-driven migration occurs and its effect on the planetary system, in particular the rate at which planetesimals are scattered into the inner regions. We consider that such scattered material has the potential to resupply an exozodi on long time-scales. We investigate whether the rate at which material is transported inwards is sufficient to sustain the observed exozodi. We start in Section 2 by discussing our simulations. In Section 3, we discuss the migration of the outer planet in our simulations and in Section 4 the manner in which this migration increases the rate at which material is scattered into the inner regions of the planetary system. In Sections 5 and 6, we discuss the collision evolution and observations of the outer disc. Our conclusions are made in Section 7.

2 SIMULATIONS

Observations suggest that exoplanetary systems can have a wide variety of architectures. Due to the computationally intensive nature of *N*-body simulations that include a large number of planetesimals (each of which is assigned a mass), we must limit ourselves to an interesting range of the available parameter space. We decide for simplicity to focus on solar-like planetary systems. For want of a better example, we follow the presumed primordial belt in the Solar system (Gomes et al. 2005; Tsiganis et al. 2005), we consider a planetesimal belt that runs from 15 to 30 au and, as in our Solar system, place several planets interior to the belt. It is the outer of these planets that we envisage migrating outwards through the planetesimal belt. The interior planets are necessary for planetesimals to be scattered by this outer planet inwards to the regions where an exozodi might be observed. Fig. 1 illustrates a planetary system of this configuration and the manner in which an exozodi may be produced. Although an exozodi may be produced by a planetary system of a different configuration, for the purposes of this study we limit ourselves to this architecture.

A further complication arises due to the fact that the observed exozodi results from the emission due to small dust grains, yet due to the computationally intensive nature of our *N*-body simulations, we can only follow the evolution of ‘large’ planetesimals. We consider the observed small dust to be a lower limit on the total mass of material that must be transported inwards in order to sustain an exozodi. In our simulations, we track the mass of planetesimals that is scattered inwards. Planetesimals scattered into the inner regions of the planetary system evolve due to a variety of processes,

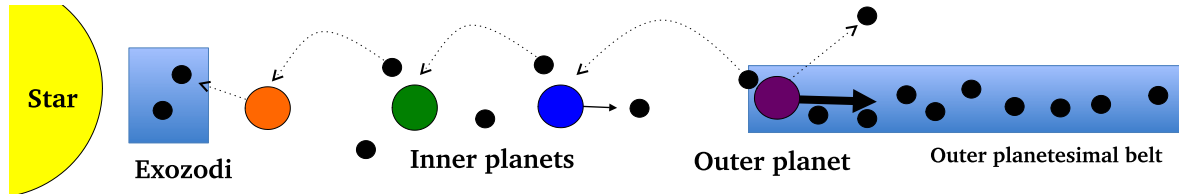


Figure 1. A diagram (not to scale) to illustrate the scattering of planetesimals by an outer planet, that leads to an exchange of angular momentum and the outward migration of that planet. Some of the scattered particles are ejected, whilst some are scattered into the inner planetary system, where they interact with the inner planets. This scattering leads to a flux of material into the exozodi region.

including collisional processing, sublimation and radiative forces, for example Nesvorný et al. (2010) suggest the spontaneous disruption of comets, driven by sublimating volatiles, produces the zodiacal dust in our Solar system. We envisage that these lead to the conversion of the scattered planetesimals to the observed small dust grains, with some efficiency, but exact modelling of this problem is complex and not the focus of the current work. Thus, we use the rate at which planetesimals are scattered interior to 3 au as a proxy for the maximum rate at which the observed exozodi could be replenished. This is a reasonable approximation, as long as the lifetime of the planetesimals in this region is shorter than the time bin (100 Myr) that we use to count the arrival of planetesimals. We acknowledge the limitations of this technique, in particular the fact that planetesimals may be scattered on to eccentric orbits that enter and leave the region interior to 3 au without depositing significant mass.

All the initial conditions of our simulations are detailed in Table 1. Although our simulations model the gravitational effects of the planetesimals on the planet, we neglect interactions between the

planetesimals themselves. This is unlikely to be important, although it has been suggested that it could lead to some viscous spreading of the disc (Ida et al. 2000; Levison et al. 2011; Raymond et al. 2012). In order to simplify our initial conditions, we chose to place five equal-mass planets between the pristine inner edge of the outer belt $a_{\text{pl.out}} = 15$ and 5 au, at semimajor axes of 5, 6.6, 8.7, 11.4 and 15 au, where the ratio between adjacent pairs is constant at $\frac{a_2}{a_1} = 1.3$. This purely arbitrary choice enables us to investigate the dependence on a few key parameters, for example the separation of the planets and their masses.

Our simulations were run using the hybrid integrator found in the MERCURY package (Chambers 1999). Any planetesimals that are scattered beyond 10 000 au are considered to be ejected, and we track the number of particles that are scattered within 3 au of the star. A timestep of 200 d ensures good energy conservation down to 3 au (see appendix A of Raymond et al. 2011).

We run both simulations with test particles (no mass) and simulations in which the particles are assigned a mass of $m_{\text{part}} = M_{\text{belt}}/N$, where M_{belt} is the total mass of the planetesimal belt, which we

Table 1. Initial conditions of our simulations.

Planet		
Outer planet semimajor axis	$a_{\text{pl.out}}$	15 au
Planet semimajor axes	a_{pl}	5,6.6,8.7,11.4,15 au
Planet semimajor axes*	a_{pl}	5,8.7,15 au
Planet masses $M_{\text{belt}}(0) = 10 M_{\oplus}$	M_{pl}	2, 5, 10, 15, 20, 30 M_{\oplus}
Planet masses $M_{\text{belt}}(0) = 100 M_{\oplus}$	M_{pl}	50, 70, 100, 130, 165, 465 M_{\oplus}
Planet density ($M_{\text{pl}} < 0.5 M_{\oplus}$)	ρ	3.9 g cm ⁻³
Planet density ($0.5 < M_{\text{pl}} < 10 M_{\oplus}$)	ρ	5.5 g cm ⁻³
Planet density ($11 < M_{\text{pl}} < 49 M_{\oplus}$)	ρ	1.6 g cm ⁻³
Planet density ($50 < M_{\text{pl}} < 500 M_{\oplus}$)	ρ	1.3 g cm ⁻³
Ratio between planet periods	$\frac{a_2}{a_1}$	1.3,1.5,1.7
Inner pair of planets		[10 M_{\oplus} , 5 M_{\oplus}], [30 M_{\oplus} , 5 M_{\oplus}], [100 M_{\oplus} , 5 M_{\oplus}], [100 M_{\oplus} , 30 M_{\oplus}], [30 M_{\oplus} , 100 M_{\oplus}]
Planetesimal belt		
No. of particles	N	2500
Planetesimal mass	no mass	0
Planetesimal mass	mass	$M_{\text{belt}}(0)/N$
Total mass	$M_{\text{belt}}(0)$	10, 100 M_{\oplus}
Surface density	Σdr	$\propto r^{-1} dr$
Semimajor axes	a_{pp}	15–30 au
Eccentricity	e_{pp}	0–0.01
Inclinations	i_{pp}	0–0.1°
Longitude of ascending node	Ω_{pp}	0°–360°
Longitude of pericentre	Δ_{pp}	0°–360°
Free anomaly	J_{pp}	0°–360°
Other parameters		
Stellar mass	M_*	1 M_{\odot}
Ejection radius	r_{out}	10 000 au
Inner radius	r_{in}	3 au

*For planet masses higher than $M_{\text{pl}} = 40 M_{\oplus}$.

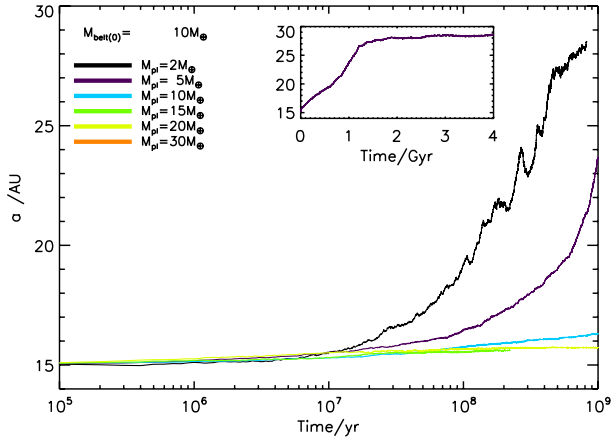


Figure 2. The change in the semimajor axis of the outer planet in our simulations, for planets of various masses embedded in a disc of initial mass $10 M_{\oplus}$. The inset shows the continued evolution of the $5 M_{\oplus}$ planet until it reaches the outer edge of the belt. The detail in the behaviour of the $2 M_{\oplus}$ planet is affected by the limited resolution of our simulations, particularly at late times. Migration is stalled for planet masses greater than $10 M_{\oplus}$.

initially set to either $M_{\text{belt}}(0) = 10 M_{\oplus}$ or $M_{\text{belt}}(0) = 100 M_{\oplus}$, and N is the number of particles used in the simulation ($N = 2500$). The no mass simulations provide a comparison to the mass simulations, in which exchange of angular momentum and migration of the planets is possible. The choice of number of particles and the 1 Gyr run-time for simulations were made in order to minimize the computational resources required. We note here that typical lifetimes of FGK stars can be much longer than the 1 Gyr run-time of our simulations; however, given that each of the mass simulations takes about 2 months to run for 1 Gyr¹, we satisfy ourselves with simulating this limited portion of the system’s evolution. The resolution is sufficient if the ratio of the planet mass to the particle mass is greater than 600 (Kirsh et al. 2009), which applies to our simulations for planet masses above $2.4 M_{\oplus}$ ($M_{\text{belt}}(0) = 10 M_{\oplus}$) or $24 M_{\oplus}$ ($M_{\text{belt}}(0) = 100 M_{\oplus}$). This means that caution must be taken in assessing the results of the simulations with a $2 M_{\oplus}$ planet and $M_{\text{belt}}(0) = 10 M_{\oplus}$.

3 PLANET MIGRATION

3.1 The conditions for migration

In some, but not all of our simulations, the outer planet migrates outwards. We focus initially on the simulations with an initial belt mass of $M_{\text{belt}}(0) = 10 M_{\oplus}$. Fig. 2 shows the change in semimajor axis of the outer planet during our simulations. The migration rate depends on the relative mass of the planet to the surface density of the disc. We find three important trends in the migration rate:

- (i) migration of the outer planet is outwards;
- (ii) migration is stalled for planets above a critical mass, M_{stall} ;
- (iii) lower mass planets migrate at faster rates.

We are able to estimate the critical mass, M_{stall} to be about $10 M_{\oplus}$ for $M_{\text{belt}}(0) = 10 M_{\oplus}$, when the inner planets are arranged in the manner of our simulations. This mass is critically important. If migrating planets are required to produce exozodi, M_{stall} tells us the

maximum mass a planet can have and still migrate. The $5 M_{\oplus}$ planet is the best example of migration that we found in our simulations. The $2 M_{\oplus}$ planet also provides a good example of migration, but the small ‘blips’ in its migration at later times can be accredited to the limited resolution of our simulations.

We can readily understand the observed trends. The planet migrates due to an exchange of angular momentum as it interacts with planetesimals in a zone surrounding the planet. If these planetesimals are exterior to the planet, they generally have a z -component of their specific angular momentum ($H_z = \sqrt{a(1-e^2)} \cos I$) larger than that of the planet ($H_z > H_{\text{pl},z}$), where the subscript pl refers to the planet, such that interactions tend to increase the planet’s angular momentum and its orbit spirals outwards (Gomes et al. 2004). On the other hand, planetesimals interior to the planet tend to have a z -component of their angular momentum lower than that of the planet ($H_z < H_{\text{pl},z}$), such that interactions tend to decrease the planet’s angular momentum and its orbit spirals inwards. At the start of our simulations, the planet has planetesimals exclusively exterior to its orbit, so in general it migrates outwards.

If we consider our best example of outward migration, the $5 M_{\oplus}$ planet, the left-hand panel of Fig. 3 illustrates how the surface density of the disc evolves as the planet migrates outwards. The planet scatters planetesimals inwards. If sufficient planetesimals were scattered inwards, the disc would be ‘balanced’; interactions from interior and exterior planetesimals would cancel one another. However, this scattering is not sufficient. As can be clearly seen in the figure, an imbalance in surface density remains, which ‘fuels’ the planet’s outward migration.

Migration is not always sustained in this manner. Higher mass planets, such as the $30 M_{\oplus}$ shown in the right-hand panel of Fig. 3, scatter more planetesimals, in a potentially more ‘violent’ manner, but tend to migrate less due to their increased inertia. This tends to ‘symmetrize’ the disc and more importantly it carves out a deep gap in the disc around the planet, as can clearly be seen in Fig. 3. This stalls the planet’s migration, as the planet runs out of ‘fuel’.

Previous work (Kirsh et al. 2009; Bromley & Kenyon 2011; Ormel et al. 2012) has seen planet migration stall at high planet masses. Ormel et al. (2012) derive an analytic condition for a planet’s migration to be stalled, by comparing the viscous stirring time-scale (an approximation to the time-scale to clear the planet’s encounter zone of material) to the migration time-scale, under the approximation of a dispersion-dominated disc, such that random velocities dominate encounters, rather than Keplerian shear. This occurs for (equation 58 of Ormel et al. (2012) in our notation):

$$M_{\text{pl}} \gtrsim M_{\text{stall}} = 23 \Sigma(a) a^2 e_0, \quad (1)$$

where e_0 is the eccentricity of the planetesimals at the planet’s semimajor axis, a and $\Sigma(a)$ the local disc surface density. The results of our simulations confirm the existence of such a limit, although we note here that the value of M_{stall} is not exact and depends on the properties of the disc, that are in turn influenced by the planet and its migration.

Fig. 4 illustrates diagrammatically the conditions for migration, according to equation (1), with the simplifying assumption that the disc eccentricity at the location of the planet is $e_0 = 0.1$, although the dashed lines indicate the variation in this line between discs with eccentricities of $e_0 = 0.01$ and $e_0 = 0.5$.

An additional regime in which very low mass planets migrate, but have little influence on the disc is also plotted on Fig. 4. This regime was not probed by our simulations due to our limited resolution. An analytic condition for this is derived in Ormel et al. (2012, equation 52 written in our notation) the minimum planet mass required to

¹ On a single core on *fofino*, the Service Commun de Calcul Intensif de l’Observatoire de Grenoble (SCCI) supercomputer.

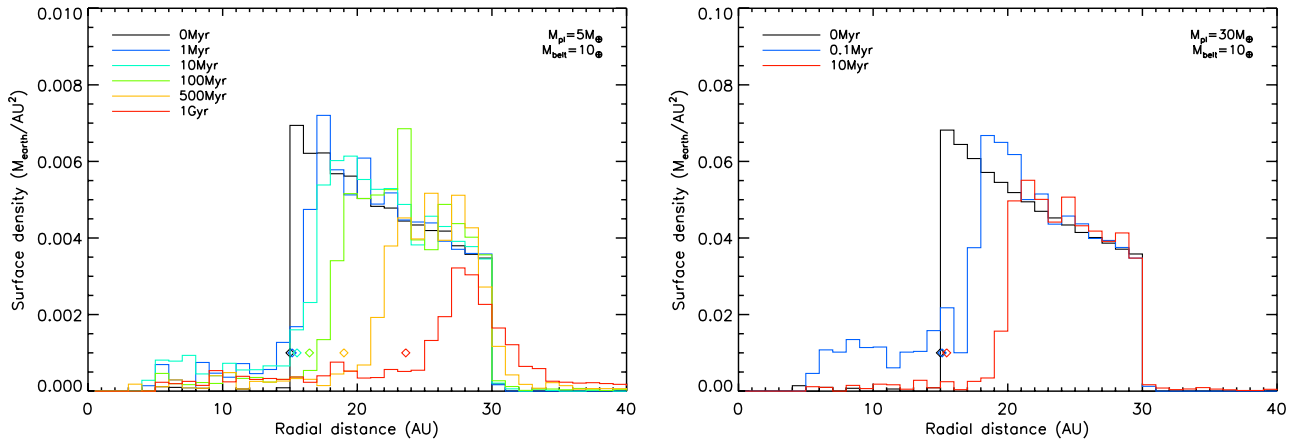


Figure 3. The evolution of the surface density of planetesimals in the belt, calculated by tracking the number of planetesimals with semimajor axes in bins of width 1 au ($N_i(a)$), such that $\Sigma(a) = \sum_i N_i(a) m_{\text{part}} / (\pi (r_{\text{bin, out}}^2 - r_{\text{bin, in}}^2))$, where $r_{\text{bin, in}}$ and $r_{\text{bin, out}}$ refer to the inner and outer edges of the bin. The diamonds show the position of the outer planet at the different epochs. The left-hand plot shows how the $5 M_{\oplus}$ planet clears the disc, whilst migrating through it. The right-hand plot shows how the $30 M_{\oplus}$ planet clears the zone surrounding it of material and migrates no further. Both plots consider an initial disc mass of $10 M_{\oplus}$.

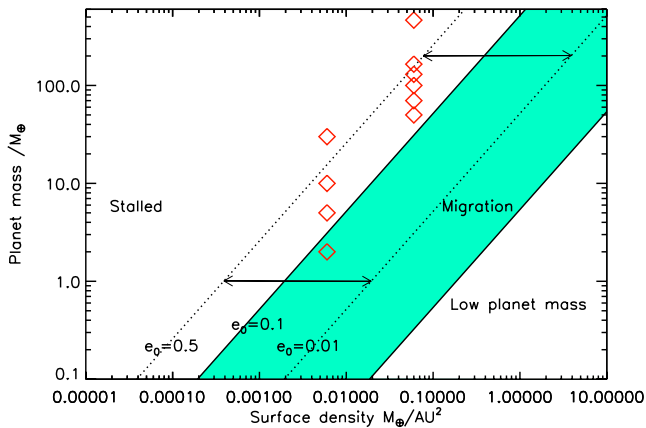


Figure 4. The range of planet masses for which the analytic criterion of Ormel et al. (2012) find that migration should occur is shown by the green shaded region (equations 1 and 2), assuming that the disc eccentricity is $e_0 = 0.1$ and $a = 15$ au. The dashed lines indicate the variation in the upper boundary (equation 1) with the disc eccentricity, between $e_0 = 0.01$ (the start of our simulations) and $e_0 = 0.5$. The red diamonds indicate the initial conditions of our simulations, although it should be noted that the surface density rapidly decreases with time as the planet scatters material away. This plot should be applied with caution as the properties of the disc are liable to change due to the planet's migration and these approximations are only valid for a single planet embedded in a dispersion-dominated disc.

excite a noticeable eccentricity, high enough to sustain an imbalance between the disc interior and exterior to the planet:

$$M_{\text{pl}} \lesssim 24 \Sigma(a) a^2 e_0^3. \quad (2)$$

Below this planet mass, we assume that the planet does not scatter sufficient planetesimals in order to produce an exozodi. Thus, whilst very low mass planets may migrate through outer discs on long time-scales, they are unlikely to be the origin of exozodiacal dust.

The initial conditions for our simulations have been added as diamonds to Fig. 4, which could in theory be used to predict their migration. However, we note here that the disc surface density and eccentricity will evolve as the simulation progresses, such that in general the red points move left on Fig. 4, whilst the upper boundary moves left and up. This means that the planet may occupy different

migration regimes. In addition, perturbations from other planets affect the migration. Thus, in practice, this plot can only be used to estimate the initial migration regime for a given planet and disc.

3.2 The influence of the inner planets

In order to produce an exozodi by scattering material inwards from an outer belt, several planets are required to cover the large distance between the outer belt and the exozodi. A planet that is sufficiently close to the migrating planet in order to scatter any particles, which are scattered in its direction, is sufficiently close to affect the migration of the outer planet. The planet's migration is slowed by interactions with particles that it has previously scattered interior to its orbit. An inner planet can remove these particles, thus, increasing the rate, or triggering, the outer planet's migration. Inner planets can also increase the eccentricity of the planetesimals in the disc. Both of these factors can lead to substantial changes in the rate at which the outer planet migrates.

Fig. 5 shows the difference in the migration of the outer planet, when we changed the initial separation of the planets. This is for a fixed planet mass of $5 M_{\oplus}$ and initial belt mass of $10 M_{\oplus}$. This figure shows that migration occurs at higher rates if the planets are more closely packed. This is due to the increased influence of the inner planet. This figure illustrates a potentially important bias in our simulations. Our choice of planet separation moved the $5 M_{\oplus}$ planet from a regime in which its migration was stalled (when the inner planets are far away or do not exist) to a regime in which its migration is self-sustained on Gyr time-scales. This adds another difficulty in predicting exactly which planets migrate using equation (1) or Fig. 4.

3.3 Increasing the surface density of the disc

A similar set of simulations were run for an initial belt mass of $100 M_{\oplus}$ (see Section 2). According to equation (1), a higher disc surface density, means that higher mass planets will migrate. For our choice of inner planetary system with planets at 5, 6.6, 8.7, 11.4 and 15 au, with $\frac{a_2}{a_1} = 1.3$, equal mass planets of greater than $40 M_{\oplus}$ are likely to become unstable, as their separation is less than $8 R_{\text{H}}$, where R_{H} is the Hill radius, given by $R_{\text{H}} = \frac{a_1 + a_2}{2} \left(\frac{m_{\text{pl},1} + m_{\text{pl},2}}{3 M_{*}} \right)^{1/3}$, where

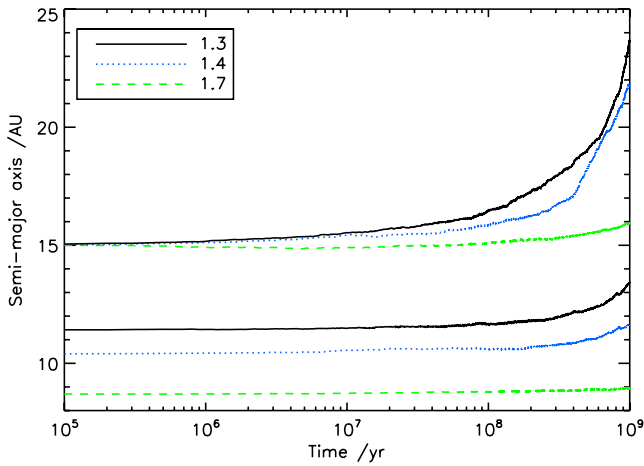


Figure 5. The change in semimajor axis of the outer two $5M_{\oplus}$ planets, in simulations with an initial disc mass of $10M_{\oplus}$, but where the initial separation of the planets is increased from $\frac{a_2}{a_1} = 1.3$ (five planets) to $\frac{a_2}{a_1} = 1.4$ (four planets) to $\frac{a_2}{a_1} = 1.7$ (three planets), as described in Section 2. The closer the planets, the faster the migration.

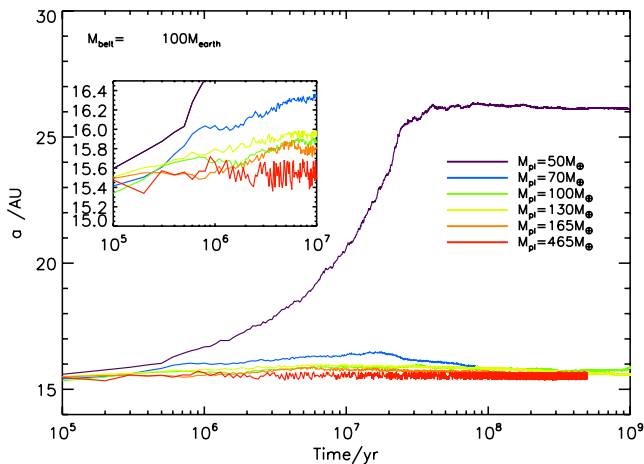


Figure 6. The same as Fig. 2, but for an initial belt mass of $100M_{\oplus}$. The inset shows the first 10^7 yr, to illustrate that most of the planets migrate, but only a small distance. Note that in order to ensure stability the inner planetary system only contained three planets with $\frac{a_2}{a_1} = 1.7$, which has a critical influence on the migration (see discussion in Section 3.3 for further details). Please note that if the planet was not migrating *after* ~ 100 Myr, due to the computationally intensive nature of the simulations, not all were evolved for 1 Gyr.

$m_{pl,1}$ and $m_{pl,2}$ are the mass of the planets and M_* the mass of the star. We, therefore, chose to increase the separation of the planets. This decision has a critically important effect on the migration rates, as discussed in the previous section (Section 3.2). This effect must be considered when analysing the migration rates of the outer planets in these simulations, shown in Fig. 6.

In these simulations, many of the planets initially migrate (see inset on Fig. 6 for details, noting that the planets all started at 15 au), but their migration is commonly stalled, as the planets clear the zone surrounding them of material. Only the 50 and $70M_{\oplus}$ planets continue to migrate on longer time-scales, and then only for tens of millions of years. The migration of the $50M_{\oplus}$ is stalled as it reaches the outer edge of the belt. In a wider belt, this migration may well have continued on longer time-scales. The migration of the $70M_{\oplus}$ stalls as the planet scatters particles and reduces the surface density

of the disc. In fact, the planet has scattered sufficient material interior to its orbit, that its migration restarts in an inwardly direction.

We note here the dependence of the migration discussed in Section 3.2 on the architecture of the inner planetary system. Our arbitrary choice may play a critical role in our results. It may be possible to change this architecture in a manner such that migration continues on Gyr time-scales even in these high surface density discs.

3.4 The width of the belt

In our simulations, we chose to consider a belt width of 15 au. This choice is relatively arbitrary and planetesimal belts in exoplanetary systems may well be substantially wider. Migration may be sustained on longer time-scales in a wider belt. Thus, the width of the belt is critically important in ascertaining whether or not migration is sustained. The $50M_{\oplus}$ planet in a belt of initial mass, $M_{\text{belt}}(0) = 100M_{\oplus}$, whose migration was stalled after ~ 30 Myr, would have continued to migrate for ~ 100 Myr if the belt were approximately 100 au wide (and migration continued at approximately the same rate). Nonetheless, it would be difficult to sustain migration on Gyr time-scales. On the other hand, the migration of the $5M_{\oplus}$ planet through the belt of $M_{\text{belt}}(0) = 10M_{\oplus}$ stalls after ~ 3 Gyr, for this width belt, somewhat less than the typical main-sequence lifetime of solar-type stars, that can be up to tens of Gyr.

On an interesting aside, we note that for a sufficiently wide belt, the outer planet can migrate such that it becomes separated from the inner planets. In this case, a stable belt may form between the two planets. The conditions for this to occur were discussed in detail in Raymond et al. (2012).

4 SCATTERING OF PLANETESIMALS TOWARDS THE INNER PLANETARY SYSTEM

4.1 The benefits of planet migration

Our hypothesis is that a planet that migrates outwards continuously encounters new material in the disc that it can scatter inwards. Migrating planets, therefore, continue to scatter planetesimals on long time-scales. We suppose that it is these planetesimals scattered into the inner regions of the planetary system that have the potential to replenish a dusty, exozodi. Therefore, we focus on the fate of planetesimals scattered inwards from an outer belt, for simplicity, ignoring any planetesimals that may reside initially between the planets.

We track the rate at which particles are scattered inwards, recording the first time at which a particle enters the region interior to 3 au. Scattering depends on the architecture of the inner planetary system in a complicated manner. Given that the parameter space required in order to explore this dependence fully is large, without a full investigation, our strongest conclusions result from a comparison of the scattering rates between the mass and nomass simulations. The aim of this comparison is to remove dependence on the planet masses, semimajor axes, etc. and focus solely on the difference caused by the migration of the outer planet(s). The inner planetary system does, however, have a critical effect on the migration of the outer planet (see Section 3.2 for more details), which is hidden in this comparison.

Fig. 7 shows the number of particles that enter the region interior to 3 au, in time bins of width 100 Myr, for the mass simulations divided by the same number for the nomass simulations, for the low

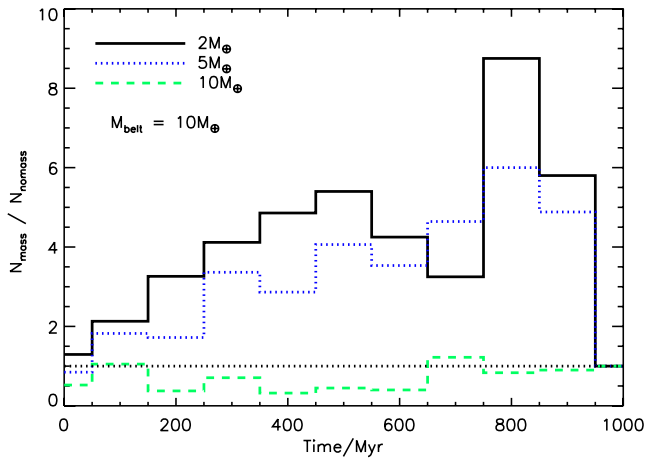


Figure 7. The ratio between the number of particles scattered into the inner planetary system (<3 au) with (*mass*) and without (*nomass*) migration of the outer planet, in the simulations with an initial disc mass of $10M_{\oplus}$. Only those planets that migrated are shown, 2 and $5M_{\oplus}$, with $10M_{\oplus}$ for comparison. On short (<100 Myr) time-scales, the non-migrating planets scatter more material inwards, but the migrating planets continue to scatter material inwards on Gyr time-scales.

surface density outer belts ($M_{\text{belt}}(0) = 10M_{\oplus}$). The two outer planets that migrated, with $M_{\text{pl}} = 2$ and $5M_{\oplus}$, clearly scatter significantly more material inwards, than in the *nomass* simulations where there was no migration. The $10M_{\oplus}$ whose migration was not significant, showed little difference in scattering behaviour between the *mass* and *nomass* simulation. This provides good evidence that migration can increase the transport of material inwards, in a manner that has the potential to produce an exozodi.

Similar behaviour is seen for the higher surface density discs ($M_{\text{belt}}(0) = 100M_{\oplus}$), except that here migration only continued for <35 Myr (see Fig. 8). During migration, however, the same increase in scattering rates for the *mass* simulations, compared to the *no mass* simulations is seen.

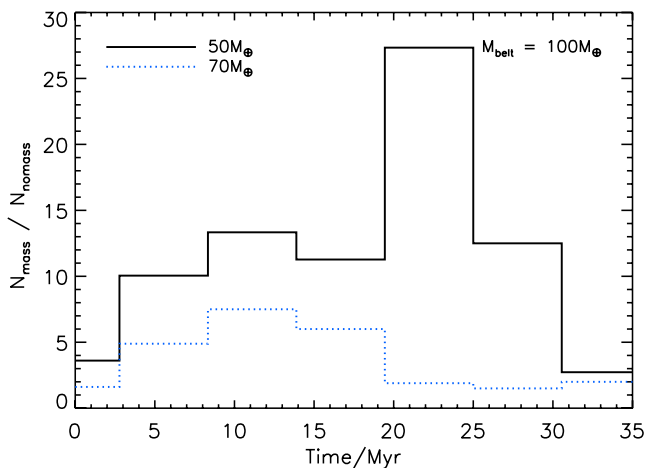


Figure 8. The same as Fig. 7, except for an initial disc mass of $100M_{\oplus}$, and a bin width of 10 Myr. The $50M_{\oplus}$ migrated for ~ 30 Myr and the $70M_{\oplus}$ for ~ 10 Myr (see Fig. 6); hence, the plot only shows the behaviour on these shorter time-scales.

4.2 Is the mass flux sufficient to produce an exozodi?

This is a very difficult question, given that observationally neither the mass in dust, nor its lifetime is well constrained, in addition to which, as discussed in Section 2, the conversion of the large planetesimals scattered inwards to the small dust grains observed is complex and difficult to constrain. First, considering the observations, a few examples exist where attempts have been made to estimate the mass in dust. τ Ceti is one such example, for a solar-type star. The mass of dust is estimated to be $\sim 10^{-9}M_{\oplus}$ in di Folco et al. (2007) in grains between $0.1\mu\text{m}$ and 1.5mm in size. This is estimated assuming that the dust forms a disc; the width, height, composition, size distribution and mass of which are estimated using Bayesian analysis. The collisional lifetime of this dust is estimated to be of the order of weeks to years, such that the dust must be resupplied at a rate of at least $\sim 10^{-9}M_{\oplus}\text{yr}^{-1}$, but maybe as high as $5 \times 10^{-8}M_{\oplus}\text{yr}^{-1}$ in order to sustain the observed levels, where the estimate should not be considered to be accurate to within more than an order of magnitude.

Secondly, we consider the exact manner in which the dust is resupplied. Collisions between larger bodies are likely to play an important role, as well as sublimation and radiative forces. The mass in planetesimals scattered inwards will be dominated by larger bodies. It may be that eventually most of this mass is converted to the observed small dust, but more likely the conversion is not 100 per cent efficient. In fact, it would not be unreasonable that some planetesimals, scattered interior to 3 au on highly eccentric orbits, leave the inner regions of this planetary system, without depositing any mass.

We, therefore, acknowledge that the exact mass flux required to sustain an observable exozodi is difficult to estimate and may vary from system to system. We improve our estimation of the scattering rate by using a time bin (100 Myr) to count the arrival of planetesimals which is large compared to their predicted lifetime in the inner regions. We consider $\sim 10^{-9}M_{\oplus}\text{yr}^{-1}$ to be an absolute lower limit on the mass in planetesimals scattered inwards and highlight that more material may be required to sustain an observable exozodi.

4.2.1 Low surface density discs

We start by plotting the rate at which planetesimals are scattered inwards in our ‘low-density’ simulations ($M_{\text{belt}}(0) = 10M_{\oplus}$). Fig. 9 shows these rates, again calculated by counting the number of particles that enter the region interior to 3 au in time bins of width 100 Myr. The two important simulations on this plot are those in which the outer planet migrated, i.e. $M_{\text{pl}} = 2M_{\oplus}$ and then $M_{\text{pl}} = 5M_{\oplus}$. The scattering rates calculated with migration (black open squares and blue open triangles) should be compared to those in which migration did not occur (blue filled triangles and black filled squares). The critical point to take from this figure is that the migrating planets continue to scatter material inwards at rates that do not decrease significantly with time.

As discussed above, it is difficult to estimate whether or not these scattering rates are sufficient to sustain an exozodi. The key point is that the migrating planets retain the scattering rates approximately an order of magnitude higher than without migration of the outer planet. The scattering rates for the migrating planets are above the absolute minimum mass flux required to sustain an exozodi of $10^{-9}M_{\oplus}\text{yr}^{-1}$. They are not, however, sufficiently higher than the absolute minimum that it is clear that these planetary systems would lead to detectable exozodi. We note here, also, that the scattering process needs to be fairly efficient at transporting material inwards in

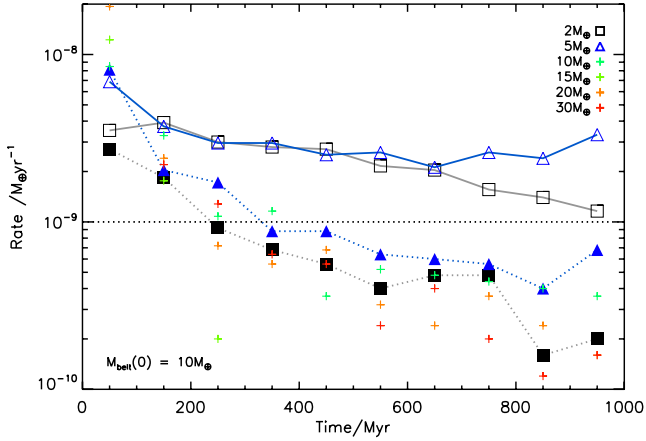


Figure 9. The rate at which material is scattered interior to 3 au in the simulations with $M_{\text{belt}}(0) = 10 M_{\oplus}$, calculated by counting the number (mass) of particles that entered this region in time bins of width 100 Myr. To provide an indication the $2 M_{\oplus}$ ($5 M_{\oplus}$) planet scattered ~ 600 (~ 800) particles interior to 3 au, respectively. The mass simulations where migration occurred ($M_{\text{pl}} = 2, 5 M_{\oplus}$), shown by the open blue triangles and open black squares, should be compared to the simulations without migration, no mass, shown by the filled squares and triangles. The rest of the simulations, where the outer planet’s migration was insignificant, are shown by the small crosses for comparison. The horizontal line indicates a scattering rate of $10^{-9} M_{\oplus} \text{ yr}^{-1}$, our estimate of the minimum rate required to sustain exozodi.

order to sustain an exozodi. For 1 Gyr, $1 M_{\oplus}$ is required to sustain $10^{-9} M_{\oplus} \text{ yr}^{-1}$, i.e. 10 per cent of the total initial mass of this low-mass belt.

4.2.2 The effect of the inner planetary system on the scattering rates

As noted in Section 3.2, the architecture of the inner planetary system can significantly affect the migration of the outer planet. It also has an important impact on the efficiency at which particles are scattered inwards to the exozodi region. These effects are difficult to disentangle from one another and from the results of our simulations. In Section 3.2, we noted that the migration rates of the outer planet decrease with the separation of the innermost planets, specifically the planet *directly* interior to the migrating planet. This leads to a decrease in the rate at which planetesimals are scattered inwards, as shown by Fig. 10. In fact, with $\frac{a_2}{a_1} = 1.7$, the outer planet did not migrate very far at all, and therefore, its scattering rate is similar to the no mass simulations.

We also tested the effect of changing the mass of the innermost pair of planets (see Section 2 for details). This did not significantly affect the migration rates, but an increase in the masses of the innermost planets, increased the rate at which planetesimals scattered inwards reached the exozodi region (< 3 au). Fig. 10 shows this dependence.

4.2.3 Higher surface density discs

The higher surface density discs ($M_{\text{belt}}(0) = 100 M_{\oplus}$) provide an interesting comparison. First, we note that a higher total disc mass, means that there is a higher mass of material that could be scattered inwards, and thus, in general, with or without migration of the outer planet, scattering rates are higher. This is because of the increased mass in the outer planet’s chaotic zone. As the chaotic zone is

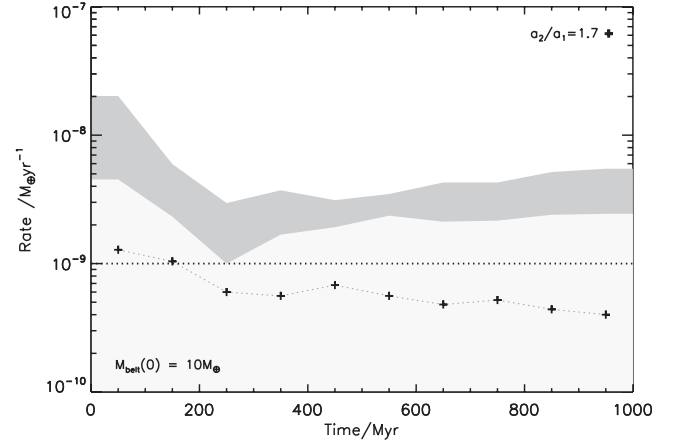


Figure 10. The same as Fig. 9, but only for an outer planet mass of $M_{\text{pl}} = 5 M_{\oplus}$, with $M_{\text{belt}}(0) = 10 M_{\oplus}$. The shaded are indicates the effect of changing the separation of the inner planets from $\frac{a_2}{a_1} = 1.3$ to $\frac{a_2}{a_1} = 1.5$, or the masses of the inner pair of planets to $[10 M_{\oplus}, 5 M_{\oplus}]$, $[30 M_{\oplus}, 5 M_{\oplus}]$, $[100 M_{\oplus}, 5 M_{\oplus}]$, $[100 M_{\oplus}, 30 M_{\oplus}]$ and $[30 M_{\oplus}, 100 M_{\oplus}]$. For $\frac{a_2}{a_1} = 1.7$, the planet separation is so large that no planetesimals are scattered inwards.

cleared, the scattering rates fall off steeply with time. Bonsor et al. (2012) concluded that such steady-state scattering rates, without migration of the outer planet, are generally insufficient to sustain an exozodi. Our *new* results are more favourable, first, because the outer belt that we use is closer to the star (15 au rather 60 au), and secondly, our choice of a constant ratio of semimajor axes to separate the planets, increases the scattering rates, as resonances with the second outermost planet overlap with resonances with the outer planet in the zone just exterior to the outer planet’s chaotic zone, destabilising this region.

Now, we assess whether migration of the outer planet has a significant effect on the scattering rates, as shown in Fig. 11. The $50 M_{\oplus}$ planet migrated rapidly outwards, reaching the edge of the belt in < 50 Myr. The entire belt is rapidly depleted of material and the scattering rates drop off very quickly at late times.

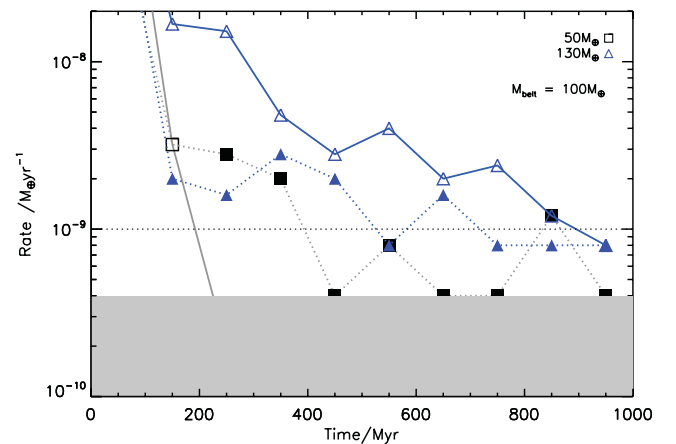


Figure 11. The same as Fig. 9, except for $M_{\text{belt}}(0) = 100 M_{\oplus}$. We show the $M_{\text{pl}} = 50 M_{\oplus}$, as example of a simulation in which the outer planet migrated and $M_{\text{pl}} = 130 M_{\oplus}$, as an example of a simulation where there was little migration of the outer planet. The solid lines and diamonds indicate the mass simulations and the dotted lines and triangles, the no-mass simulations. The grey shaded area indicates the limit of our resolution, given by the scattering of one particle in a time bin of width 100 Myr.

The outward migration of the $130 M_{\oplus}$ in the mass simulations, on the other hand, only lasted for a short time period and the planet moved a small distance (see the inset in Fig. 6). This migration, however, is sufficient to increase the total reservoir of material available to the planet, as both its interior and exterior chaotic zones are now full of planetesimals. It is, therefore, able to scatter material inwards at an increased rate, on longer time-scales. This explains why the scattering rates are higher for the mass simulations than the nomass simulations.

These results suggest that with a higher surface density disc, scattering rates might be high enough to sustain a detectable exozodi for young (<500 Myr old) stars, but that scattering rates start to fall below the minimum around 1 Gyr. This is independent of large-scale migration of the outer planet, although potentially helped by initial conditions in which the outer planet's interior and exterior chaotic zones are full (as in the mass simulation, where the planet migrated a small distance). We now note that, as discussed in the following section, collisional evolution can be important and reduce the mass available in the outer disc with time. We also question whether or not it is realistic to consider such massive discs of planetesimals, given that it is unlikely that such a massive disc did not form planets; $100 M_{\oplus}$ of solid material, would correspond to $\sim 10\,000 M_{\oplus} \sim 0.03 M_{\odot}$ of gas, comparable to the typical disc mass inferred from sub-mm observations (Andrews & Williams 2007).

4.2.4 Width of the belt

The results presented here suggest that one way to maintain high scattering rates is for the outer planet to continue to migrate outwards. The outward migration of the planet is generally stalled because the surface density of the disc reduces, either because the planet has scattered all the material away (the planets whose migration stalls initially), the disc has collisionally eroded (see Section 5) or because the planet reaches the outer edge of the belt. Self-stirring of the disc may, however, lead to the spreading of the disc over time and could in principle re-start the migration.

Our choice of a belt width of 15 au in this work was fairly arbitrary and it is very likely that exoplanetary systems could have wider or narrower belts. Fig. 12 confirms the decrease in scattering rates in one of our simulations ($M_{\text{pl}} = 5 M_{\oplus}$ and $M_{\text{belt}}(0) = 10 M_{\oplus}$), where

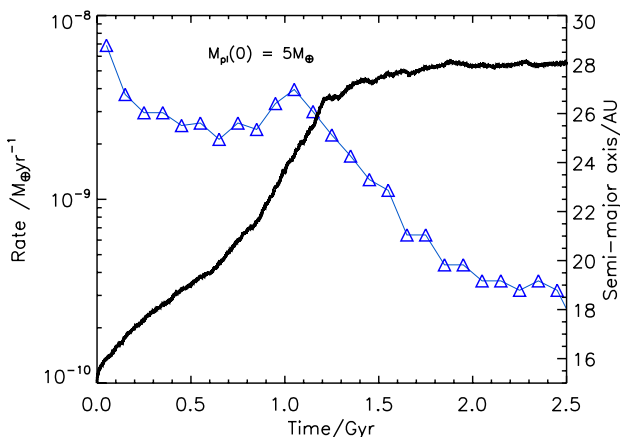


Figure 12. The scattering rates drop after the $5 M_{\oplus}$ planet reaches the edge of the belt, with $M_{\text{belt}}(0) = 10 M_{\oplus}$. The blue triangles show the scattering rates, and the black line the outward migration of the outer planet in this simulation.

the migration of the outer planet stopped as it reached the outer edge of the belt.

Due to the computationally intensive nature of the simulations, they were only continued for 1 Gyr, yet the main-sequence lifetime of many solar-type stars can be as long as 10 Gyr, and exozodi are observed around stars that are this old (Absil et al. 2013). This places another important limit regarding the ability of a planetary system to sustain an exozodi. The older the star, the wider the belt required, or the slower the migration of the outer planet, such that migration can continue on sufficiently long time-scales. For our best example of the $5 M_{\oplus}$ planet that migrated ~ 15 au in ~ 1.5 Gyr, assuming that migration continues at approximately the same rate, migration could continue for 5 Gyr in a 50 au wide belt. Such a wide belt, retaining the same surface density, would have a total mass of $\sim 100 M_{\oplus}$, such that only 5 per cent of the belt mass must be transported to the exozodi region to retain a delivery rate of $10^{-9} M_{\oplus} \text{ yr}^{-1}$ for 5 Gyr. There is good observational evidence for the existence of such wide belts (e.g. Müller, Löhne, & Krivov 2010; Churcher, Wyatt, & Smith 2011a; Bonsor et al. 2013a).

4.2.5 Summary

Our simulations show that sufficient mass in planetesimals can be scattered inwards from an outer planetary system, given sufficiently efficient conversion of the material scattered interior to 3 au into the observed small dust grains. In a disc with sufficiently high surface density this can occur without migration of the planets, but only for a limited time period. Fig. 11 shows that in some cases this can be up to 500 Myr–1 Gyr. For a disc with a lower surface density, the outward migration of the outer planet into an outer planetesimal belt is required. Our simulations show that this migration can be sustained for an appropriate configuration of the outer planet mass and the surface density of the disc in the region of the planet. The planet mass should not be so high that it clears the zone of material surrounding it before it has migrated across this zone, but at the same time sufficiently massive that its migration continues at a slow enough rate that it only reaches the outer edge of the belt after Gyr. We saw this for the $5 M_{\oplus}$ planet in our simulations with $M_{\text{belt}}(0) = 10 M_{\oplus}$. The belt must be sufficiently wide that migration is not halted as the planet reaches its outer edge.

5 COLLISIONAL EVOLUTION OF THE OUTER BELT

5.1 The decrease in scattering rates

Our work so far has ignored the collisional evolution of the outer belt. This is critically important. As the mass of the belt is reduced by collisions, the mass of material that can be scattered inwards decreases and it becomes harder to sustain an inward scattering rate high enough to sustain an exozodi. In addition to this, if the disc mass decreases sufficiently, a low-mass planet that was migrating through the disc may clear its encounter zone of material faster than it migrates, such that its migration is stalled. On the other hand, collisions may themselves scatter some planetesimals into the encounter zone of the outer planets.

A simple approximation can be used to assess the collisional evolution of the belt. We assume that it depends *inversely* on the collision time-scale of particles in the belt, t_c , such that

$$\frac{dM_{\text{belt}}}{dt} = -\frac{M_{\text{belt}}}{t_c}. \quad (3)$$

Wyatt et al. (1999), Wyatt & Dent (2002) and Wyatt et al. (2007a) derive an expression for this collisional lifetime, assuming that all bodies smaller than D_{\min} are removed by radiation pressure, that the mass of the disc is dominated by the largest bodies of diameter, D_C , and that the disc contains a Dohnanyi size distribution of bodies (Dohnanyi 1969) with a power index of $\frac{7}{2}$ (Tanaka, Inaba, & Nakazawa 1996). It also assumes that particles can be catastrophically destroyed by particles significantly smaller than themselves, that the disc is *narrow* (of width dr), does not spread radially and that its collisional evolution started at a time $t = 0$ (i.e. no delayed stirring, e.g. Mustill & Wyatt 2009; Kennedy & Wyatt 2010). The collisional lifetime of the disc is then given by (equation 16 of Wyatt 2008):

$$t_c = 1.4 \times 10^{-9} \frac{r(\text{au})^{13/3} \left(\frac{dr}{r}\right) Q_D^* (\text{Jkg}^{-1})^{5/6} D_C(\text{km})}{M_{\text{belt}}(M_{\oplus}) M_* (M_{\odot})^{4/3} \langle e \rangle^{5/3}} \text{Myr}, \quad (4)$$

where r the central radius of the belt of width dr , Q_D^* the dispersal threshold, D_C the size of the largest body in the disc, M_* the stellar mass and $\langle e \rangle$ is the average eccentricity of particles in the disc, assumed to be constant. Values for Q_D^* and D_C can be determined from observations of the population of debris discs orbiting FGK stars. Kains, Wyatt, & Greaves (2011) find $Q_D^* = 3700 \text{ Jkg}^{-1}$ and $D_C = 450 \text{ km}$, with the disc eccentricity fixed at $\langle e \rangle$ fixed at 0.05, noting the degeneracy between these parameters. Thus, the collisional lifetime of the discs considered here, with $r = 22.5 \text{ au}$ and $dr = 15 \text{ au}$, is 4.2 Gyr (420 Myr) for belts of initial mass $10 M_{\oplus}$ ($100 M_{\oplus}$). In this manner, the mass remaining in these discs after 1 Gyr of evolution can be estimated, using $M_{\text{belt}}(t) = \frac{M_{\text{belt}}(0)}{1 + \frac{t}{t_c}}$, to find $M_{\text{belt}}(1 \text{ Gyr}) = 8 M_{\oplus}$ ($M_{\text{belt}}(1 \text{ Gyr}) = 30 M_{\oplus}$). In a similar manner after 10 Gyr of evolution, $M_{\text{belt}}(10 \text{ Gyr}) = 3 M_{\oplus}$ ($M_{\text{belt}}(10 \text{ Gyr}) = 4 M_{\oplus}$). Noting that these numbers ignore any dynamical depletion of the belt. These numbers were calculated using a very simplistic approximation, and more sophisticated models suggest that the collisional evolution may be slower than suggested here (e.g. Löhne, Krivov, & Rodmann 2008; Gáspár, Rieke, & Balog 2013; Kral, Thébault, & Charnoz 2013).

As the mass in the outer belt is collisionally eroded there is less material available to be scattered inwards. Thus, it becomes more difficult to scatter sufficient material inwards to sustain an exozodi. We can consider the effect of this on our results by reducing the ‘mass’ of each particle, actually representative of a small sample of particles, by an appropriate factor, i.e. after 1 Gyr, 0.8 for the $M_{\text{belt}} = 10 M_{\oplus}$ simulations and 0.3 for the $M_{\text{belt}} = 100 M_{\oplus}$ simulations and after 10 Gyr, 0.3 for the $M_{\text{belt}} = 10 M_{\oplus}$ simulations and 0.04 for the $M_{\text{belt}} = 100 M_{\oplus}$ simulations. This is not self-consistent and does not take into account the potential reduced migration of the planet as the outer belt mass is collisionally reduced. This correction factor was not applied to Fig. 9, but would act to decrease the scattering rates at late times. In fact, on sufficiently long time-scales the disc mass will tend to the same value, regardless of the initial conditions (Wyatt et al. 2007a). This collisional evolution adds to the uncertainties in determining whether a specific scattering rate is sufficient to produce an exozodi.

5.2 Does collisional evolution stall the migration?

In Section 3, we discussed how migration stalls for planet masses above a critical mass (M_{stall}), that depends on the surface density (or mass) of the disc. As the disc collisionally evolves, a given planet could switch from a regime in which it migrates, to one

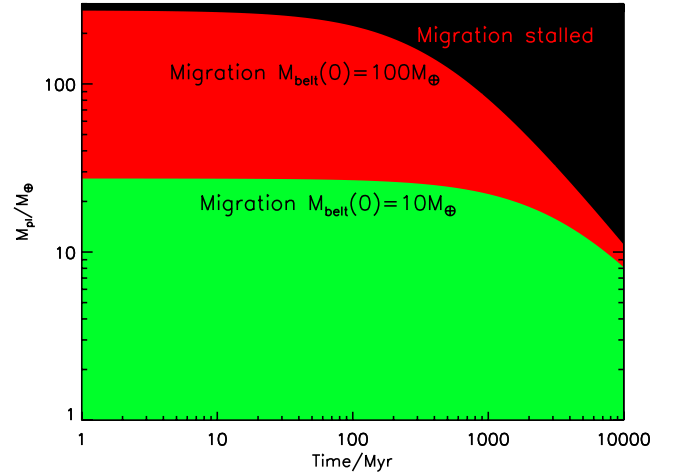


Figure 13. The critical planet mass above which planetesimal-driven migration stalls, calculated using equations (1) and (4) for the evolution of the belt mass, assuming a rather excited disc with $e_0 = 0.5$, centred on $r = 22.5 \text{ au}$ and ignoring any change in the belt width or radius. Although the exact application of equation (1) to our simulations is not clear, this plot is nonetheless indicative of the difference made by the collisional evolution of the outer belt. For the higher surface density disc, migration can be stalled relatively early due to the collisional depletion of the outer belt.

in which its migration is stalled. We estimate where this might occur by considering the analytic formulae for M_{stall} , derived by Ormel et al. (2012) (equation 1), fixing the surface density of the disc at $\Sigma(a) = \frac{M_{\text{belt}}}{\pi(a_{\text{belt,out}}^2 - a_{\text{belt,in}}^2)}$. Fig. 13 plots the evolution of the critical planet mass above which migration stalls, following the collisional evolution of the disc according to equations (3) and (4). This neglects any dynamical evolution in the disc mass, change in the disc radius or width and takes a high value for the disc eccentricity ($e_0 = 0.5$), in order to estimate the maximum effect of the collisional evolution. Although equation (1) may not provide an exact description of the behaviour in our simulations, this plot is still indicative of the influence of collisional evolution on our simulations. Fig. 13 shows that whilst for the low surface density disc ($M_{\text{belt}}(0) = 10 M_{\oplus}$), collisional evolution is not significant and does not greatly change the migration of the outer planets, with masses less than $10 M_{\oplus}$, that migrated in our simulations. On the other hand, for the higher surface density discs ($M_{\text{belt}}(0) = 100 M_{\oplus}$), collisional evolution can be of significant importance. For example, even in a very wide belt, the migration of a $50 M_{\oplus}$ outer planet would be stalled after 1 Gyr, merely because of the decrease in the disc surface density due to collisions, regardless of whether it reached the edge of the belt or not. A $200 M_{\oplus}$ planet would have its migration stalled after only 100 Myr.

6 OBSERVATIONS OF THE OUTER BELT

An intriguing question, of critical importance to the interpretation of observations of exozodi, regards whether or not an outer belt must be detected in order for it to supply an exozodi. Some planetary systems have both exozodi detections and outer belts, whilst for others no outer belt is detected. Absil et al. (2013) find a tentative correlation between what they term ‘cold’ excess and exozodi detection, or *K*-band excess, which they find for 4/11 FGK having previously detected outer belts, compared to 1/17 FGK stars, where there is no evidence for an outer belt. Ertel et al. (in preparation), on the other hand, find no significant correlation within their PIONIER survey,

nor in a combination of the PIONIER and CHARA data. Thus, the relationship between outer belts (cold excesses) and exozodi remains unclear.

We present in this work examples of planetary systems in which the outward migration of an outer planet, driven by the scattering of planetesimals, can sustain an exozodi. Noting that many other planetary systems may exist where this scenario could work, we focus on the results of our simulation of a $5 M_{\oplus}$ planet migrating outwards into a belt of mass $M_{\text{belt}}(0) = 10 M_{\oplus}$. The detectability of the outer disc depends on the collisional erosion of large planetesimals that leads to the production of small dust grains. Exact predictions for this process and the detectability of a debris disc from knowledge only of the evolution of the large planetesimals, as in our case, are very difficult (Wyatt 2008; Booth et al. 2009; Raymond et al. 2012). In a similar manner, it is difficult to extrapolate from the observed small dust and determine the total mass of the disc, or the size of the largest body (e.g. Greaves et al. 2004; Wyatt et al. 2007b; Wyatt 2008). Rather than making many vague approximations, we instead consider a simple approximation and track the approximate mass of material that remains in a stable disc ($e < 0.02$ and $a_{\text{pl}}(1 + \delta a_{\text{chaos}}) < a < 30$ au). After 1 Gyr, this has fallen to $1 M_{\oplus}$, not taking into account any collisional erosion of the disc.

A good example of a debris disc detected in a similar position to the belts considered in this work is τ Ceti, a nearby (3.65pc), old (10 Gyr) sun-like star. The total mass of the disc (in bodies up to 10 km in size) is estimated to be around $\sim 1.2 M_{\oplus}$ (Greaves et al. 2004). Comparing this to our simulation, we find that our disc is still just about detectable after 1 Gyr, but it is unlikely to remain detectable for long after this. A more realistic system is unlikely to remain detectable even for this long, as collisions will erode the disc further than our naive estimate, and τ Ceti is significantly closer to the Sun than many stars with exozodi detections in Absil et al. (2013, 3.65pc, compared to up to 40 pc). We, therefore, envisage the possibility that a disc of this type continues to sustain an exozodi, without itself being hard to detect with current instruments.

Clearly these rough approximations would change depending on the exact properties of the outer belt in any given planetary system, and the exact detection properties of the instrument used to search for ‘cold’ excess. The width of the outer belt is critically important in determining its detectability. We do not, therefore, intend to make any precise predictions regarding whether or not a detection of outer belt, makes it more likely that the exozodi is sustained by this mechanism. Instead, we merely highlight that a correlation between the presence and outer discs and exozodi is not required in order for the outer belt to sustain an exozodi.

7 DISCUSSION AND CONCLUSIONS

High levels of dust observed in the inner regions of planetary systems, known as exozodi, are difficult to explain, particularly in old (> 100 Myr) planetary systems. In this work, we investigate whether the migration of an outer planet, driven by the scattering of planetesimals, can explain these observations. We show that in principle the outward migration of the planet maintains a reasonably high mass flux of planetesimals scattered inwards to the inner regions of the planetary systems, as long as the planet continues to migrate outwards. We hypothesize that these planetesimals could resupply the observed exozodi. An example of this scenario, applied to the specific constraints of the Vega planetary system is illustrated in Raymond & Bonsor (2014). Tight constraints on the architecture of

the planetary system, however, are required in order for this scenario to work.

First, we re-iterate that the constraints on how much material must be transported inwards are poor, incorporating the poor observational constraints on the mass of small dust grains, the poor theoretical constraints on the lifetime of this dust and the poorly constrained conversion of large planetesimals to small dust grains. We estimate the minimum mass flux required and show that this can be produced by planetesimals scattered inwards by planets, either if the outer planet migrates into a low surface density outer disc whilst the migration continues, or at early (< 500 Myr) times for higher surface density discs, independent of migration of the outer planet (although the efficiency of the scattering was increased in our simulations by separating the inner planets by constant ratios of their orbital periods).

We show that the migration of an outer planet can be sustained on Gyr time-scales, and longer in planetary systems with wide outer belts. Whether or not a planet migrates, and how fast it migrates, depends critically on the mass of the planet and the surface density of the disc. Migration stalls if the planet mass is sufficiently high that it clears the zone surrounding it of material before it has migrated across it. In order to sustain migration on long time-scales, the best candidates are the slow migration of planets with masses just below the critical limit at which their migration is stalled, and in discs of lower surface density. The lower surface density of the disc also avoids problems with collisional depletion of the disc material stalling the migration. Wide belts are required if the migration is to continue for the full 10 Gyr main-sequence lifetime of a Sun-like star. This suggests that the ‘old’ (several Gyr) planetary systems with detectable exozodi, in this scenario, would originally have had wide planetesimal belts, although these belts may by now have been cleared. It also suggests that if the frequency of planetary systems with narrow planetesimal belts is higher than that with wider planetesimal belts, there would be an increased probability of planetesimal-driven migration producing exozodi around younger stars, in stark contrast to the lack of age dependence in the exozodi phenomenon found in the observations of Absil et al. (2013). On the other hand, our estimations in Section 6 suggest that the lack of a correlation between the presence of an exozodi and a detection of a cold, outer belt does not rule out the ability of planetesimal-driven migration to supply the observed exozodi.

To summarize, we have presented simulations that illustrate the manner in which the outward migration of a planet into a planetesimal belt could increase the rate at which planetesimals are scattered inwards and thus, has the potential to produce detectable exozodi, even in old (> 10 Gyr) planetary systems.

ACKNOWLEDGEMENTS

AB acknowledges the support of the ANR-2010 BLAN-0505-01 (EXOZODI). SNR thanks the CNRS’s PNP programme and the ERC for their support. SNR’s contribution was performed as part of the NASA Astrobiology Institute’s Virtual Planetary Laboratory Lead Team, supported by the NASA under Cooperative Agreement no. NNA13AA93A. Computations presented in this paper were performed at the Service Commun de Calcul Intensif de l’Observatoire de Grenoble (SCCI) on the supercomputer funded by Agence Nationale pour la Recherche under contracts ANR-07-BLAN-0221, ANR-2010-JCJC-0504-01 and ANR-2010-JCJC-0501-01. CWO acknowledges support for this work by NASA through Hubble Fellowship grant no. HST-HF-51294.01-A awarded by the Space Telescope Science Institute, which is operated by the Association

of Universities for Research in Astronomy, Inc., for NASA, under contract NAS 5-26555.

REFERENCES

- Absil O. et al., 2006, *A&A*, 452, 237
 Absil O. et al., 2013, *A&A*, 555, A104
 Andrews S. M., Williams J. P., 2007, *ApJ*, 659, 705
 Bonsor A., Augereau J.-C., Thébault P., 2012, *A&A*, 548, A104
 Bonsor A., Kennedy G. M., Crepp J. R., Johnson J. A., Wyatt M. C., Sibthorpe B., Su K. Y. L., 2013a, *MNRAS*, 431, 3025
 Bonsor A., Raymond S., Augereau J.-C., 2013b, *MNRAS*, 433, 2938
 Booth M., Wyatt M. C., Morbidelli A., Moro-Martín A., Levison H. F., 2009, *MNRAS*, 399, 385
 Bromley B. C., Kenyon S. J., 2011, *ApJ*, 735, 29
 Chambers J. E., 1999, *MNRAS*, 304, 793
 Churcher L., Wyatt M., Smith R., 2011a, *MNRAS*, 410, 2
 Churcher L. J. et al., 2011b, *MNRAS*, 417, 1715
 Czechowski A., Mann I., 2010, *ApJ*, 714, 89
 Defrère D. et al., 2011, *A&A*, 534, A5
 di Folco E. et al., 2007, *A&A*, 475, 243
 Dohnanyi J. S., 1969, *J. Geophys. Res.*, 74, 2531
 Dominik C., Decin G., 2003, *ApJ*, 598, 626
 Eiroa C. et al., 2013, *A&A*, 555, A11
 Fernandez J. A., Ip W.-H., 1984, *Icarus*, 58, 109
 Gáspár A., Rieke G. H., Balog Z., 2013, *ApJ*, 768, 25
 Gomes R. S., 2003, *Icarus*, 161, 404
 Gomes R. S., Morbidelli A., Levison H. F., 2004, *Icarus*, 170, 492
 Gomes R., Levison H. F., Tsiganis K., Morbidelli A., 2005, *Nature*, 435, 466
 Greaves J. S., Wyatt M. C., Holland W. S., Dent W. R. F., 2004, *MNRAS*, 351, L54
 Ida S., Bryden G., Lin D. N. C., Tanaka H., 2000, *ApJ*, 534, 428
 Jackson A. P., Wyatt M. C., 2012, *MNRAS*, 425, 657
 Kains N., Wyatt M. C., Greaves J. S., 2011, *MNRAS*, 414, 2486
 Kennedy G. M., Wyatt M. C., 2010, *MNRAS*, 405, 1253
 Kennedy G. M., Wyatt M. C., 2013, *MNRAS*, 433, 2334
 Kirsh D. R., Duncan M., Brasser R., Levison H. F., 2009, *Icarus*, 199, 197
 Kral Q., Thébault P., Charnoz S., 2013, *A&A*, 558, A121
 Lawler S. M. et al., 2009, *ApJ*, 705, 89
 Lebreton J. et al., 2013, *A&A*, 555, A146
 Levison H. F., Morbidelli A., 2003, *Nature*, 426, 419
 Levison H. F., Morbidelli A., Tsiganis K., Nesvorný D., Gomes R., 2011, *AJ*, 142, 152
 Lisse C. M., Chen C. H., Wyatt M. C., Morlok A., Song I., Bryden G., Sheehan P., 2009, *ApJ*, 701, 2019
 Lisse C. M. et al., 2012, *ApJ*, 747, 93
 Löhne T., Krivov A. V., Rodmann J., 2008, *ApJ*, 673, 1123
 Malhotra R., 1993, *Nature*, 365, 819
 Müller S., Löhne T., Krivov A. V., 2010, *ApJ*, 708, 1728
 Mustill A. J., Wyatt M. C., 2009, *MNRAS*, 399, 1403
 Nesvorný D., Jenniskens P., Levison H. F., Bottke W. F., Vokrouhlický D., Gounelle M., 2010, *ApJ*, 713, 816
 Ormel C. W., Ida S., Tanaka H., 2012, *ApJ*, 758, 80
 Raymond S. N., Bonsor A., 2014, *MNRAS*, preprint ([arXiv:1403.6821](https://arxiv.org/abs/1403.6821))
 Raymond S. N. et al., 2011, *A&A*, 530, A62
 Raymond S. N. et al., 2012, *A&A*, 541, A11
 Smith R., Wyatt M. C., Haniff C. A., 2009, *A&A*, 503, 265
 Su K. Y. L. et al., 2009, *ApJ*, 705, 314
 Su K. Y. L. et al., 2013, *ApJ*, 763, 118
 Tanaka H., Inaba S., Nakazawa K., 1996, *Icarus*, 123, 450
 Trilling D. E. et al., 2008, *ApJ*, 674, 1086
 Tsiganis K., Gomes R., Morbidelli A., Levison H. F., 2005, *Nature*, 435, 459
 Wyatt M. C., 2008, *ARA&A*, 46, 339
 Wyatt M. C., Dent W. R. F., 2002, *MNRAS*, 334, 589
 Wyatt M. C., Dermott S. F., Telesco C. M., Fisher R. S., Grogan K., Holmes E. K., Piña R. K., 1999, *ApJ*, 527, 918
 Wyatt M. C., Smith R., Greaves J. S., Beichman C. A., Bryden G., Lisse C. M., 2007a, *ApJ*, 658, 569
 Wyatt M. C., Smith R., Su K. Y. L., Rieke G. H., Greaves J. S., Beichman C. A., Bryden G., 2007b, *ApJ*, 663, 365
 Wyatt M. C., Booth M., Payne M. J., Churcher L. J., 2010, *MNRAS*, 402, 657

This paper has been typeset from a $\text{\TeX}/\text{\LaTeX}$ file prepared by the author.